

PREDICTING ABSORPTION COEFFICIENT IN A HALL FROM MEASUREMENTS IN A REVERBERATION CHAMBER

PACS REFERENCE: 43.55.Fw

Authors: Noriko Nishihara and Takayuki Hidaka
Institute: Takenaka Research & Development Institute
Address: 1-5-1 Ohtsuka Inzai Chiba Japan 2701395
Tel: +81-476-47-1700
Fax: +81-476-46-6688
E-mail: nishihara.noriko@takenaka.co.jp

ABSTRACT Because of a discrepancy in sound absorptivity of acoustical materials or audience chairs measured in a reverberation chamber and that observed in a hall, accurate RT prediction of a hall has been one of the significant issues for acousticians. The main reason is caused by the difference of sound diffusivity in each room. The distribution of incident angle of sound ray onto the audience area in a room is calculated by CAD model with ray tracing technique, and compared with practical absorption measurement in two different reverberation chambers. It is found, in real halls, more sound energy incidents on the audience area at glazing angle than in reverberation chambers. Combining further consideration on existing halls by CAD modeling, the influence of the deviation in sound diffusivity in a hall on the practical absorption coefficient of a material in it and its objective measure are discussed in order to establish an accurate RT prediction method.

INTRODUCTION

In many actual situations, sound absorptivity of a material observed in a hall is substantially different from the reverberant absorption coefficient measured in a reverberation chamber, which is often assumed to have a perfectly diffused sound field. For practical design of reverberation time (RT) in a room, some empirical absorption coefficients of the interior material were published in compensation for this difference[1]. If the "effective absorption coefficient" α_{field} , that is re-defined by the Sabine equation and the RT measured in real room, of any materials or in any shape can be predicted, it comes in very useful for acousticians. This study

shows that α_{field} depends on shape of the hall, that is, physical diffusivity in it, and proposes how to predict α_{field} by numerical simulation.

NUMERICAL PREDICTION METHOD OF α_{field}

As the first step, α_{field} 's in two reverberation chambers with different shape and diffusivity were evaluated numerically. The reverberation chamber-(A) has seven walls with no parallel surfaces and has a volume of 332.8m³ and a surface area of 289.2m², in which 20 curved diffusers, each with an area of 1.8m², are randomly suspended on the basis of ISO354 [2]. The reverberation chamber-(B) has seven walls with one parallel surface: a floor and a ceiling, a volume of 178.7m³ and a surface area of 197.9m², and has no diffuser. If the sound field in a reverberation chamber is perfectly diffused and the excess attenuation by the edge effect is excluded [3], the reverberant absorption coefficient α_s of homogeneous porous material can be expressed by the statistical absorption coefficient α_{stat} , as:

$$\mathbf{a}_s = \Delta_I \cdot \mathbf{a}_{\text{stat}}, \quad (1)$$

$$\mathbf{a}_{\text{stat}} = \frac{1}{2} \int_0^{p/2} \alpha(\mathbf{q}) \cos \mathbf{q} \sin \mathbf{q} d\mathbf{q}, \quad (2)$$

where $\alpha(\theta)$ is an oblique absorption coefficient of a material and Δ_I is a correction factor derived from the modified $\cos \mathbf{q}$ law [3]. Hence, the latter's values are 1.46, 1.43, 1.38, 1.32, 1.27, 1.26 at each mid-frequency of 1/1 octave band from 125 to 4k Hz. If the sound energy incidents onto a material of unit area is given by $\cos \theta \cdot P(\theta)$, α_{field} can be defined as [4],

$$\mathbf{a}_{\text{field}} = \frac{\int_0^{p/2} \alpha(\mathbf{q}) \cos \mathbf{q} \cdot P(\mathbf{q}) d\mathbf{q}}{\int_0^{p/2} \cos \mathbf{q} \cdot P(\mathbf{q}) d\mathbf{q}}, \quad (3)$$

where $P(\theta)$ is a probability density function of the incident angles of the sound rays that impinge on the material. When the room is under perfect diffusion, the distribution $P(\theta)$ equals to $\sin \theta$ so that the α_{field} coincides with α_s . The two reverberation chambers were modeled in the computer. The $P(\theta)$ was obtained by CAD models with ray tracing technique, where the number of rays generated was 100,000 and the maximum reflection order was up to 40 or the maximum tracing time up to 2 sec. As a test material, glass wool (GW, 96kg/m³, t=50 mm, size=2,730X3,640 mm) was selected and located at the center of the floor of the model rooms. Therefore, GW area is highly absorptive, and the remaining area is perfectly reflective. Two sound sources were located at each corner of the reverberation chamber, and three receiving positions were chosen diagonally on the GW surface for the calculation. Figure 1 shows the incident energy distribution per unit area of the GW in the two reverberation chambers. One can see the distributions in chamber-(A) is nearly the same as the theoretical value so that the perfect diffusion was attained, in which the mean value and the 'skewness' parameter of the incidence angle distribution are 44° and -0.03, respectively. On the other hand, the energy distributions in the chamber-(B) deviates a little toward the grazing angle. The mean value and the skewness are 52° and 0.20, respectively. Based on the oblique absorption coefficients of the GW calculated by empirical equation [5] in Fig. 2, and the $P(\theta)$ in Fig. 1, α_{field} 's in the two chambers are compared in Fig. 3. As it turned out, α_{field} in chamber-(B) is slightly larger than that in chamber-(A). It should be noted that the differences in α_{field} (c.a. 0.07 at 125 to 500 Hz frequency bands) came from those in physical diffusion in two rooms.

Secondary, the reverberant absorption coefficients of the GW were measured in the two chambers in accordance with the procedure of ISO354 [2]. Then, the perimeter of the material was shielded by L-shape steelwares to eliminate the edge effect. As shown in Fig. 4, it can be said that there exists a systematic difference in the two absorption coefficients at lower two frequency bands, which is the same tendency as the simulated results in Fig.3. However, the discrepancy at higher frequencies seemingly came from several uncertainties at the measurement, such as accuracy of the empirical equation [4], air absorptions, and homogeneity of the material.

INCIDENT ENERGY DISTRIBUTION IN HALLS

The same numerical analysis was carried out for 11 halls in Table 1 using CAD models: six shoebox halls (AC, BC, BS, TH, VM, ZT), two distorted shoebox halls that is rectangular in plan with no parallel ceiling to the floor (TM, TO), and three fan shaped halls (OF, PS, TI). The range in volumes is 3,040 to 18,780m³. The CAD models were precisely constructed from the architectural drawings [6], but the seatings in the audience area in each hall were replaced by cuboids whose surface were made of highly absorptive material. The sound source was placed on the centerline of the hall, 3m from the front edge of the stage, at a height of 1.5m. Two receivers were chosen on the cuboids: one is near the center of the main floor but 1m off the centerline (P-101), and another is at five or six back rows of P-101 but at a distance of one third of hall width from a side wall (P-102). Figure 5 shows the typical examples of the energy distribution incident on the receivers on the cuboids as a function of the incident angle θ . The distributions of the shoebox halls that one may expect a lot of lateral reflections show larger energy above 60°. For shoebox case, the mean of the incident angel θ are 10°, in particular 20° and over for VM, greater than the perfect diffusion case, $\theta=45^\circ$. Contrariwise for the fan shaped halls, the incident energy onto the receiver is less than other shaped halls, and its distribution focuses on specific angles. As the distorted shoebox halls were recently designed regarding to initial reflections onto audiences, the incident energy is greater or equal to those of classical shoebox halls of which the ceiling is parallel to the floor. TO [7] has remarkable energy distribution near $\theta=35^\circ$ because of the huge canopy suspended above the stage, but the incident energy leans to the direction of grazing incidence. The hall widths of the 11 halls are plotted as a function of the mean of incidence angle in Fig. 6. The five classical shoebox halls (AC, BC, BS, VM, ZT) are highly correlated each other ($r=-0.94$), which means that the wider the hall width, the smaller the mean of incidence angle in these. After taking the moving-average of the distributions along the θ -axis, they were expanded into following orthogonal series:

$$\cos\mathbf{q} \cdot P(\mathbf{q}) = \sum_{n=1}^k a_n \times \sin(n \times 2\mathbf{q}) . \quad (4)$$

where a_n is a coefficient of n th term. The first two coefficients, a_1 and a_2 , are plotted as a function of the mean of incidence angle in Fig. 7. The a_1 's are almost even, while the a_2 's depend on the mean of incidence angle with high correlation ($r=0.97$). The a_1 and a_2 do not show any dependence on the hall shape. But from Fig. 8, which plots the a_3 vs. the skewness, it is speculated that the former can be an indicator for the differences of energy distributions, i.e., physical diffusivity that correlates with the sound absorption in a room accordingly.

PREDICTION OF ABSORPTION COEFFICIENTS IN HALLS

From the effective energy distributions in the previous paragraph, the α_{field} , were calculated when the plain porous materials were placed on the floor in each hall. The porous material was determined to the GW discussed above. Figure 9 shows the ratios of the α_{field} of the GW in the halls (AC, TM, TO, VM) vs. those in a reverberation chamber, i.e., α_s . VM that possesses sufficient number of lateral reflection yields a large discrepancy at low frequencies, because the oblique absorption coefficient depends on θ remarkably at low frequencies as shown in Fig. 2. Figure 10 is a plot of α_{field} of every receiver in every hall against the mean angle of incidence. The α_{field} at 125Hz highly correlates with the angle of incidence ($r=0.97$), while those at 500 and 2kHz are almost independent from 45° to 75° . In similar manner, the ratios of α_{field} vs. α_s for seated audiences in two halls (VM, TM) are given in Fig. 11. Same tendency as in Fig. 9 is observed. This finding might be another explanation why VM boasting excellent RT adopts the chairs with very lightly upholstering.

CONCLUSIONS

The effective absorption coefficients of the GW placed in two reverberation chambers with different diffusivity were measured numerically and experimentally. Both measurements were equivalent at least lower frequency band so that the assumption utilized in this study is reasonable if uncertainties at the measurement can be eliminated. The distribution of the incident sound energy onto the audience area in 11 halls was obtained by same numerical method. The distributions in halls were different from those in reverberation chambers. In particular, those of shoebox halls inclined to the direction of grazing incidence because of a lot of lateral reflections. Using this distribution function, α_{field} of ideal porous material and seated audiences in the halls were calculated and compared, and it was found that both material shows similar frequency characteristics that is determined by the hall shape. Also, new parameter that indicates the physical diffusivity in halls was proposed. In recent acoustical design methodology, it is emphasized that lateral reflections are sufficiently brought about to audiences. In that case, careful study on the seating's absorptivity especially at lower frequency is important to avoid the excessive absorption based on the physical diffusivity in that sound field.

[REFERENCES]

1. Beranek, L.L., and Hidaka T., "Sound absorption in concert halls by seats, occupied and unoccupied, and unoccupied, and by the hall's interior surfaces", J.A.S.A. 104, 3169-3177 (1998).
2. ISO 354:1985, "Acoustics-Measurement of sound absorption in a reverberation room."
3. Makita Y., and Hidaka T., "Revision of the $\cos\theta$ Law of Oblique Incident Sound Energy and Modification of the Fundamental Formulations in Geometrical Acoustics in Accordance with the Revised Law", *Acustica* 63, 163-173 (1987).
4. Nishihara N., Hidaka T., and Beranek. L.L., "Mechanism of sound absorption by seated audiences in halls", J.A.S.A. 110, 2398-2411 (2002)
5. Delany, M.E. and Bazley, E.N., "Acoustical Properties of Fibrous Absorbent Materials", *Applied Acoustics*, 3, 105-116 (1970).
6. Beranek, L. L., *Concert and Opera Halls*, (Acoust. Soc. Am. Woodbury, NY 1996).
7. Hidaka T., Beranek, L.L., Masuda S., Nishihara N., and Okano T., "Acoustical design of the Tokyo Opera City (TOC) concert hall, Japan", *J. Acoust. Soc. Am.* 107(1), 340-354, 2000.

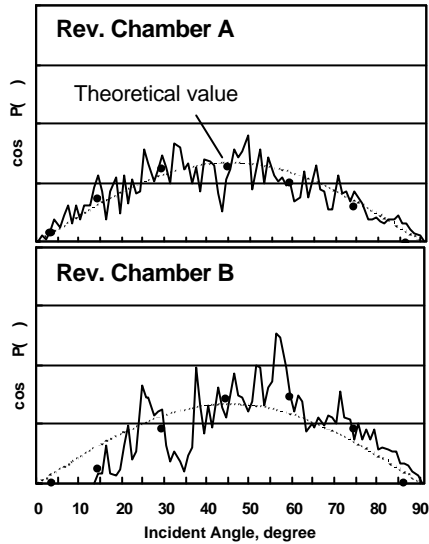


Fig. 1 Typical examples of $\cos\theta.P(\theta)$ per degree and per unit area as a function of the incident angle in the median plane. The black dots mean the average distribution at intervals of 15 degrees.

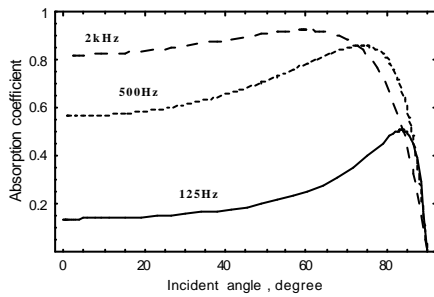


Fig. 2 Examples of $\alpha(\theta)$ for a porous layer with rigid backing at 125, 500 and 2kHz (flow resistance per cm: $65\text{gs}^{-1}\text{cm}^{-3}$; $t=50\text{mm}$) [4].

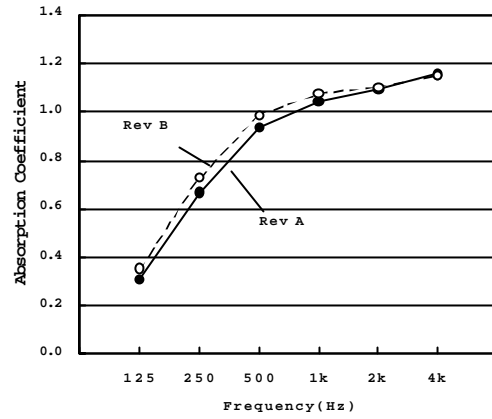


Fig. 3 Effective absorption coefficients, α_{field} , of the porous material calculated in the CAD models of reverberation chamber.

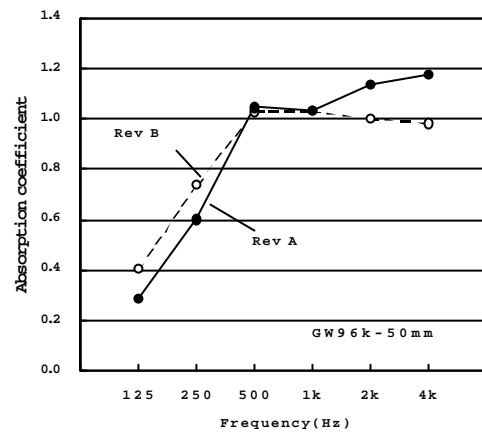


Fig. 4 Key as in Fig. 3, but for those measured in the two real reverberation chambers.

Table 1 Eleven halls used for the calculations in this study. V is room volume; N is the number of seats; Hall width of cross section shows mean value of the mainfloor.

Hall	V(m ³)	N	Hall width(m)	Hall type
AC Amsterdam, Concertgebouw	18,780	2,037	27.7	Shoe-box
BC Basel, Stadt-Casino	10,500	1,448	21.0	Shoe-box
BS Boston, Symphony Hall	18,750	2,625	22.9	Shoe-box
OF Osaka, Festival Hall	17,300	2,709	42.8	Fan shape
PS Paris, Salle Pleyel	15,500	2,386	25.6	Fan shape
TH Toyko, Hamarikyu Asahi Hall	5,800	552	15.0	Shoe-box
TI Tokyo, Iino Hall	3,040	698	20.9	Fan shape
TM Tokyo, Mitaka Arts Center	5,500	625	14.6	Distorted shoe-box
TO Tokyo, Opera City Concert Hall	15,300	1,632	20.0	Distorted shoe-box
VM Vienna, Musikvereinssaal	15,000	1,680	19.8	Shoe-box
ZT Zurich, Grosser Tonhalleaal	11,400	1,546	19.5	Shoe-box

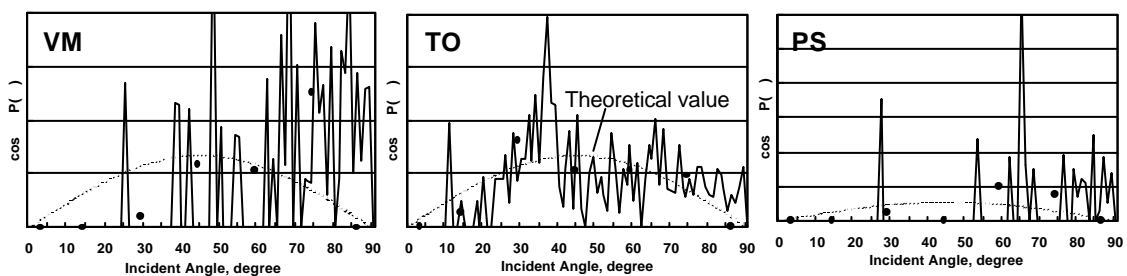


Fig.5 Key as in Fig. 1, but for the model of the halls (P-101).

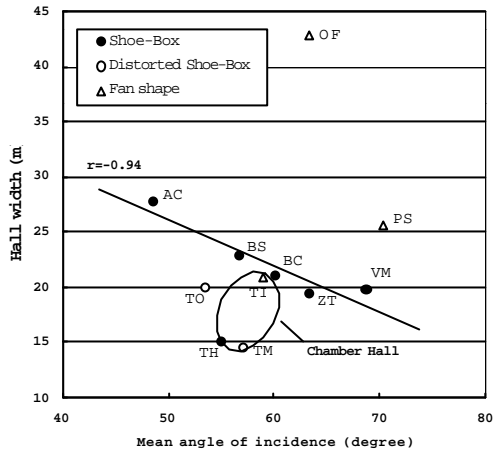


Fig. 6 Plot of the hall widths of cross section versus the mean angle of incidence onto the plain porous material placed on the seating area in the halls.

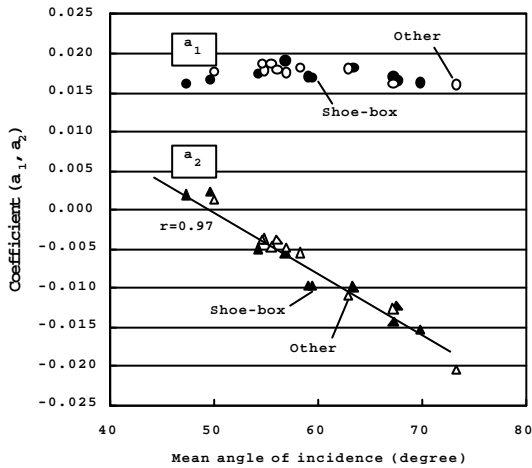


Fig. 7 Plot of coefficients of the first (a_1) and second (a_2) terms in Eq. (4) versus the mean angle of incidence onto the plain porous material placed on the seating area in the halls.

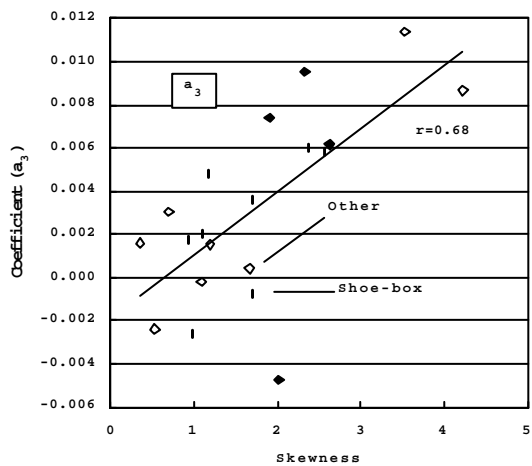


Fig. 8 Plot of the coefficients of the third term (a_3) in Eq. (4) versus the skewness, which is a parameter of asymmetric distribution.

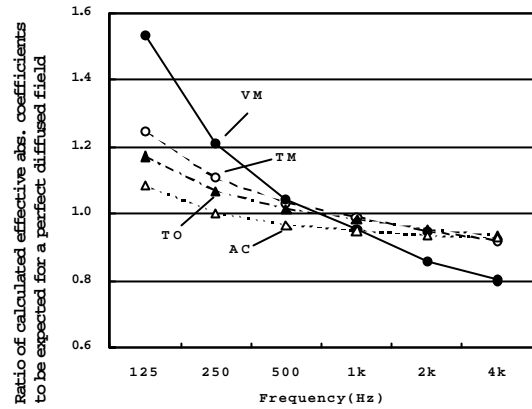


Fig. 9 Comparison of the ratios of calculated effective absorption coefficients of the porous material to be expected for a perfect diffused sound field.

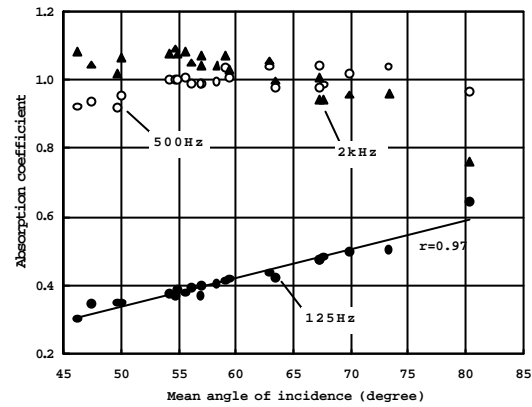


Fig.10 Plot of the α_{field} 's of the porous material calculated in the CAD models versus the mean angles of incidence onto the plain porous material placed on the seating area in the halls.

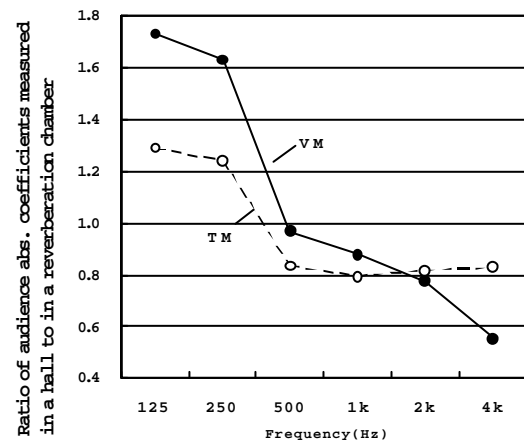


Fig. 11 Comparison of the ratios of absorption coefficients of seated audiences measured in the real halls to in the reverberation chamber.